Green Chemistry

PAPER

View Article Online
View Journal | View Issue

Check for updates

Cite this: *Green Chem.*, 2024, **26**, 3441

Composition–property relationships of choline based eutectic solvents: impact of the hydrogen bond donor and CO_2 saturation†

Ruth Dikki,[a] Vaishali Khokhar,[a] Muhammad Zeeshan,[a] Sanchari Bhattacharjee,[b] Oguz Kagan Coskun,[a] Rachel Getman‡[b] and Burcu Gurkan *[a]

Eutectic solvents are tunable for targeted applications through the functional groups in their hydrogen bond acceptor (HBA) and hydrogen bond donor (HBD) components, as well as the HBA : HBD composition ratio. This study examines the properties of choline-based eutectics containing imidazole, phenol, pyrrole-2-carbonitrile, and 1,2,4-triazole HBAs, and ethylene glycol, 1,2-propylene glycol, and ethanolamine HBDs. The viscosity, conductivity, degree of hydrogen bonding, thermal stability, and solvatochromic properties are examined as a function of HBA, HBD, and the composition. These studies revealed a predominant dependence of physical properties on the HBD and determined that the strong hydrogen bonding in phenol and imidazole-based systems lead to higher viscosities and lower conductivities – critical parameters for CO_2 capture and electrochemical conversion. The developed eutectic solvents were further evaluated in terms of their CO_2 capture capacities and electrochemical stabilities. Solvatochromic properties were found to correlate with CO_2 capacities, demonstrating the tunability of these solvents for CO_2 capture. The quantitative structure–property relationship (QSPR) analysis demonstrated the ability to predict viscosities and CO_2 capture capacities (<25% deviation) through a multi linear regression method utilizing five molecular descriptors. This work highlights the role of functionalized HBAs and HBDs in the physical, thermal, and electrochemical properties of eutectic solvents as they relate to CO_2 capture and electrochemical processes.

Received 12th December 2023,
Accepted 5th February 2024

DOI: 10.1039/d3gc04905a

rsc.li/greenchem

Open Access Article. Published on 07 February 2024. Downloaded on 4/13/2026 5:23:57 AM.
This article is licensed under a Creative Commons Attribution-NonCommercial 3.0 Unported Licence.

Introduction

Eutectic solvents are versatile liquids that present tunable properties for a variety of applications including separations, energy storage, and catalysis.[1,2] They are commonly obtained from mixtures of hydrogen bond acceptors (HBAs), such as halide salts, and hydrogen bond donors (HBDs). Deep eutectic solvents (DESs) form at the HBA : HBD eutectic composition where significant melting point depression of the resulting solvent occurs in comparison to the neat components. DESs are considered greener alternatives to volatile organic solvents because of their low volatility that originates from their high salt concentrations and strong hydrogen bonding among their constituents.[3] However, the exact 'deep' eutectic composition[4] may not be required, and the eutectic solvent composition may be suitable to take advantage of their tunable properties.[5] There are several reports of eutectic solvents displaying electrochemical and thermal stability for flow battery and CO_2 capture and conversion applications.[6–9] In particular, by functionalizing the eutectic solvent components with CO_2 reactive moieties, CO_2 selectivity and absorption capacity have been shown to improve.[10–12] When functionalizing eutectic solvents for a target application, consideration of the interplay between the physical, chemical, thermal, and electrochemical properties is important as these properties vary with molecular structure and composition.[13–16] Therefore, understanding the structure–composition–property relationship is essential in the design of eutectic solvents for targeted applications. Here, we present data for a series of choline-based eutectic solvents with demonstrated structure–composition–property relation for the example application of CO_2 capture.

Recent studies[17,18] investigating the impact of different HBA and HBD composition on the physical properties of the

[a]*Department of Chemical and Biomolecular Engineering, Case Western Reserve University, Cleveland, OH 44106, USA. E-mail: beg23@case.edu*
[b]*Department of Chemical and Biomolecular Engineering, Clemson University, Clemson, SC 29634-0909, USA*

†Electronic supplementary information (ESI) available. See DOI: https://doi.org/10.1039/d3gc04905a

‡Current address: William G. Lowrie Department of Chemical and Biomolecular Engineering, The Ohio State University, Columbus, OH 43210 USA

Open Access Article. Published on 07 February 2024. Downloaded on 4/13/2026 5:23:57 AM.
This article is licensed under a Creative Commons Attribution-NonCommercial 3.0 Unported Licence.

Table 1 Molecular structures and abbreviations of the HBAs and HBDs used in the formulation of the eutectic solvents examined. For eutectic solvents derived from choline-HBAs containing imidazole and phenol, choline dipolar ion $Ch^{\pm}$ and cation $[Ch]^{+}$ abbreviations are used due to the proton sharing existing between choline and ImH/PhOH, represented by the dashed lines. This proton sharing is observed experimentally in the synthesized $Ch^{\pm}$ImH and $Ch^{\pm}$PhOH HBAs.[22] However, it is not included in MD simulations for computational tractability, since modeling proton sharing is significantly more computationally demanding

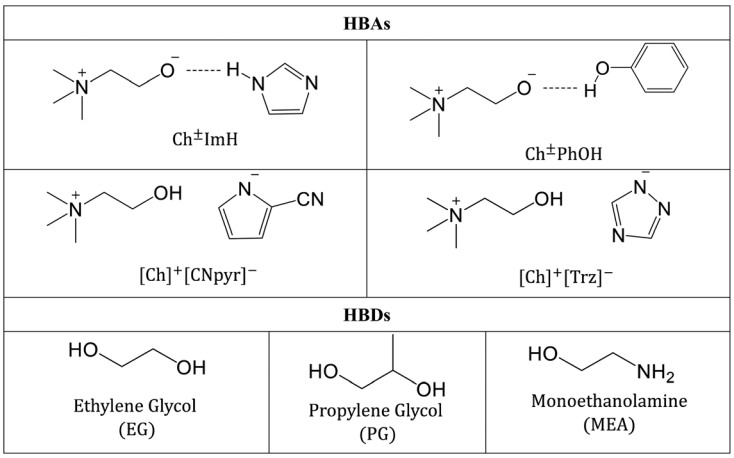

eutectic solvents reported a decrease in solvent viscosity with increase in the mole ratios of HBDs such as ethylene glycol (EG), 1,2-propylene glycol (PG), and 1,4-butanediol when choline chloride ($[Ch]^{+}[Cl]^{-}$) salt was used as the HBA. This behavior is attributed to the weakening of the HBA–HBD interactions with increased molar concentrations of the HBD. This was similarly observed in superbase and EG based eutectic solvents where increased volatility with increased EG molar ratio supports the presence of a weakened intermolecular interaction.[19] It is worth noting that this is not a universal trend for eutectic solvents; for instance in the case of glyceline DES, which is a 1 : 2 molar mixture of $[Ch]^{+}[Cl]^{-}$ and glycerol, the viscosity decreases with increasing $[Ch]^{+}[Cl]^{-}$ content up to the deep eutectic composition. This was shown to be due to the weakening of the strong hydrogen bonding between the glycerol molecules by the introduction of chloride–glycerol interactions which are weaker than the glycerol–glycerol interactions.[18] However, when HBDs such as EG are introduced to the more viscous ionic liquids (ILs), which are functional salts that melt below 100 °C, the viscosity of the resulting eutectic mixture is typically lowered.[20,21] While the reduced viscosity improves mass transport in ILs for gas separations, the introduction of a volatile component also results in lowered thermal stability. Since the chemisorbed CO_2 is conventionally released by thermal heating to regenerate the liquid, thermal stability is important for solvent cyclability and reuse in CO_2 separations by absorption-desorption techniques. Therefore, this interplay between thermal stability and viscosity should be considered when designing eutectic solvents for gas separations. Both of these properties are related to the strength of hydrogen bonding among the eutectic solvent components, which can vary widely depending primarily on the HBA anion and the type and number of hydrogen bonding sites on HBD. For CO_2 capture application, the hydrogen bonding site may also be the CO_2 binding site; therefore, these properties can further influence the CO_2 absorption capacities.

In this study, all-organic eutectic solvents based on choline HBAs with amine and alcohol functionalities, and HBDs including EG, PG, and monoethanolamine (MEA) are examined (structures shown in Table 1). Specifically, the temperature-dependent densities, viscosities, and ionic conductivities were measured in order to establish the structure–composition–property relations in these CO_2-reactive eutectic solvents. To further understand the hydrogen bonding interactions involved within these liquids, solute-solvent interactions were probed with solvatochromic dyes. The spectroscopic study offers key insights about the hydrogen bond donating/accepting ability along with the polarizability of a solvent with respect to the absorbance probes. Further, hydrogen bond statistics were computed using molecular dynamics (MD) simulations. Thermal gravimetric analysis (TGA) and differential scanning calorimetry (DSC) measurements were performed to characterize thermal behaviour and phase transitions. In order to relate the measured properties and the hydrogen bonding to CO_2 capture applications, the CO_2 absorption capacities were measured. Finally, to enable future predictions of the eutectic solvent properties, quantitative structure–property relationship (QSPR) analysis was carried out, thus establishing empirical mathematical models that only requires certain molecular descriptors of the components as input.

Result & discussion

Thermal analysis

The eutectic behavior of the solvents formed upon combining the HBAs and HBDs are confirmed by DSC. As an example,

 This journal is © The Royal Society of Chemistry 2024

Open Access Article. Published on 07 February 2024. Downloaded on 4/13/2026 5:23:57 AM.
This article is licensed under a Creative Commons Attribution-NonCommercial 3.0 Unported Licence.

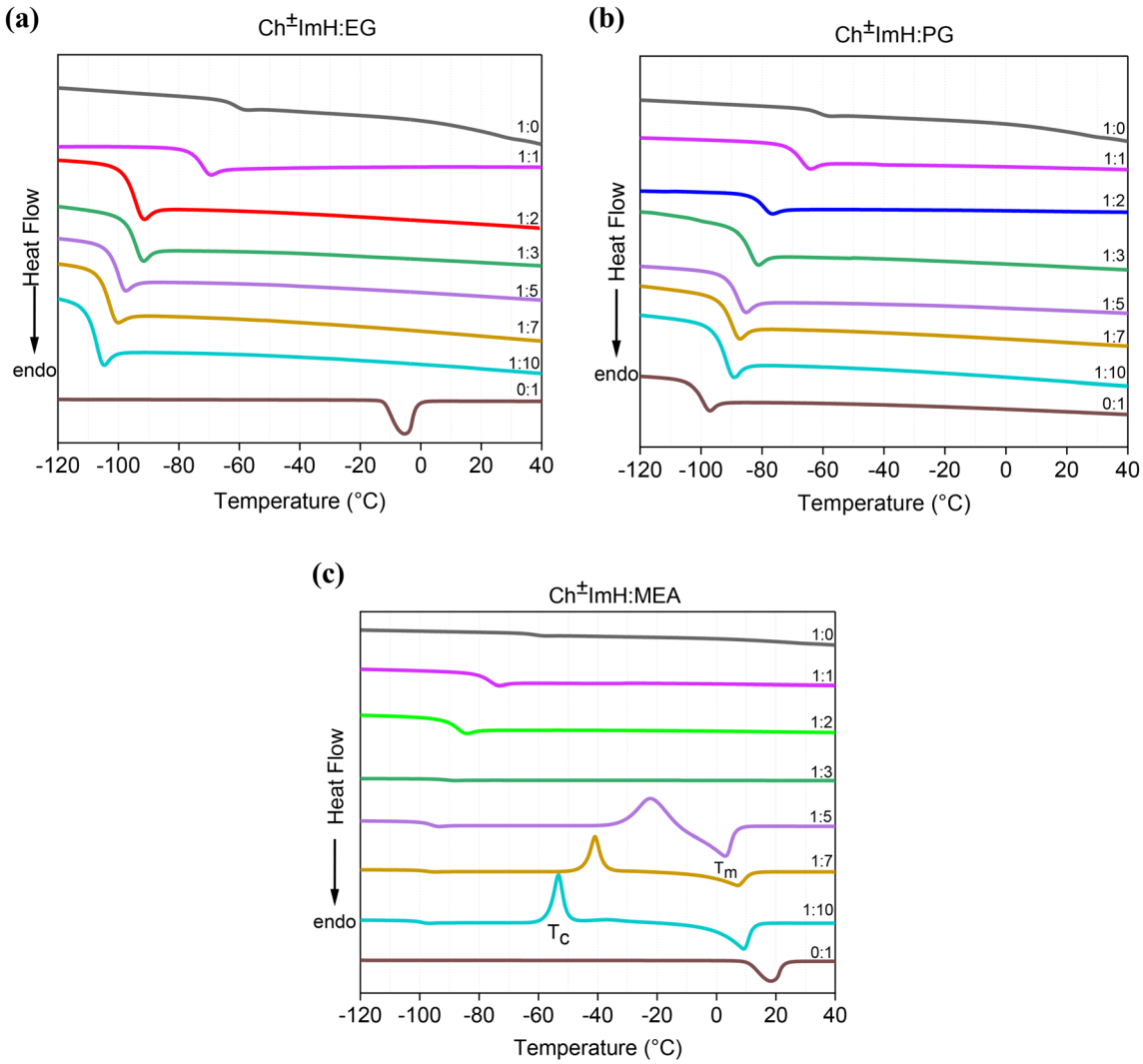

Fig. 1 DSC thermogram of Ch±ImH based solvents with different molar ratios of HBDs: EG (a), PG (b), and MEA (c). T_c and T_m represent the cold crystallization and melting peaks, respectively.

mixtures of Ch±ImH with HBDs (at 1 : 1, 1 : 2, 1 : 3, 1 : 5, 1 : 7, and 1 : 10 molar ratios of HBA : HBD) is shown in Fig. 1. Mixtures with HBD diols (those containing EG and PG), demonstrate second order glass transitions between −70 °C and −110 °C depending on the HBD content, without a clear melting peak as commonly observed for eutectic solvents.[20,21] A reduction in the glass transition temperature (T_g) is observed with increasing HBD content. A similar trend is seen for Ch±ImH : MEA mixtures when moving from 1 : 1 to 1 : 3 compositions. However, further increase in the MEA (1 : 5, 1 : 7, and 1 : 10 compositions) resulted in the appearance of cold crystallization peaks, accompanied by melting between 0 and 10 °C, thus indicating increased MEA–MEA interactions at these higher HBD compositions, along with a possible break down of the eutectic behavior. The observation of melting (T_m) and cold crystallization (T_c) peaks together with the glass transition is indicative of the formation of a semicrystalline material,[23] with an amorphous character promoted by the Ch±ImH-MEA interactions, and crystalline behavior promoted by the MEA–MEA interactions. This is indicative of a stronger hydrogen-bonding promoted by both the –NH_2 and –OH groups in the case of MEA compared to the other HBDs. A similar overview of the phase behavior was observed for the $[Ch]^+[Trz]^-$ based solvents (Fig. S1†). DSC curves for mixtures with Ch±PhOH and $[Ch]^+[CNpyr]^-$ HBAs were only examined for the 1 : 2 HBA : HBD compositions where the only clear feature was T_g (Fig. S2†). $[Ch]^+[CNpyr]^-$: MEA (1 : 2) sample demonstrated precipitation at room temperature and therefore was not studied for further characterization in the study.

It should further be noted that while the melting peaks of the neat EG and MEA are visible and consistent with literature,[24,25] the melting of PG, reported at −60 °C,[26] is absent in Fig. 1 possibly due to the rate of heating employed. PG, however, displayed a second order glass transition temperature peak around −100 °C which is lower than the known melting temperature. Therefore, the examined PG based mix-

Open Access Article. Published on 07 February 2024. Downloaded on 4/13/2026 5:23:57 AM.
This article is licensed under a Creative Commons Attribution-NonCommercial 3.0 Unported Licence.

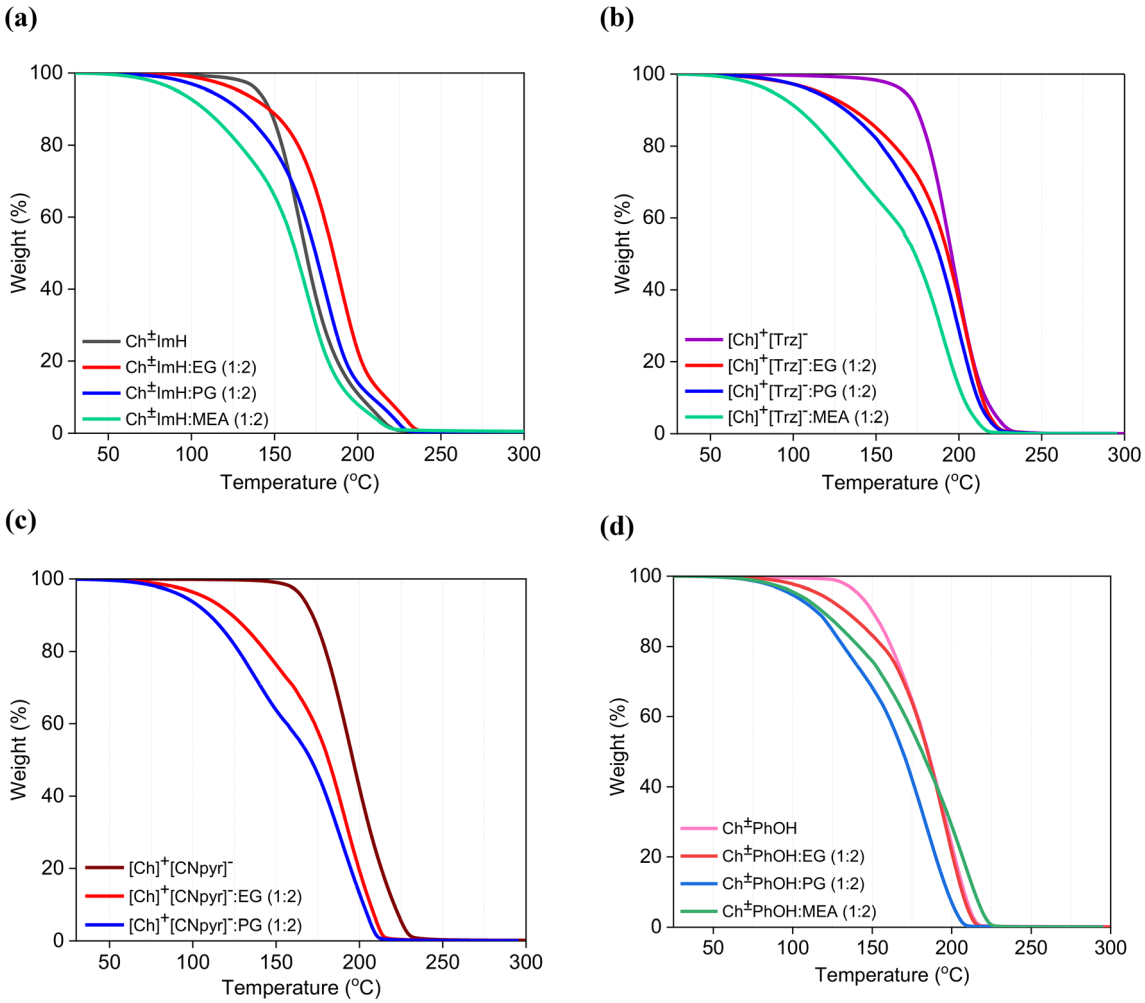

Fig. 2 TGA curves of eutectic solvents based on Ch±ImH (a), $[Ch]^+[Trz]^-$ (b), $[Ch]^+[CNpyr]^-$ (c), and Ch±PhOH (d) HBAs. The HBA : EG (1 : 2) curves are from Dikki *et al.*[22] and included here for comparison.

tures are considered eutectic solvents. Similarly, the presence of glass transition, along with the absence of melting in the DSC curves of EG and PG based mixtures indicate the absence of a defined crystal structure due to the heterogeneity in their structure and in the interactions among their constituents.

The thermal stability as it relates to the regenerability and durability of these solvents in separation applications with temperature-swing operations was examined by TGA as shown in Fig. 2. Only the systems with 1 : 2 HBA : HBD composition were examined as it is expected that further increase in the volatile HBD component would lead to lowered thermal stability.[27] The onset temperature (T_{onset}) for the eutectic solvents varied according to the boiling point (T_b) of the HBDs used while presenting no clear dependence on the stability of HBAs (see Table S1†). For instance, replacing MEA (T_b = 171 °C)[28] with PG (T_b = 187 °C)[29] and EG (T_b = 197 °C)[30] generally increased the T_{onset}. On the other hand, keeping the same HBD with varied $[Ch]^+[CNpyr]^-$ (T_{onset} = 165 °C), Ch±PhOH (T_{onset} = 141 °C), and Ch±ImH (T_{onset} = 140 °C) HBAs did not result in significant changes in the T_{onset} of the mixtures. These results suggest that it is not the thermal degradation of the HBA, but the evaporation of the HBD that dominantly controls thermal stability in these eutectics despite the existing HBA–HBD interactions. This is also apparent in Fig. S3† where the mass loss experienced by the eutectic solvents at isothermal 50 °C is reported. It is seen that for $[Ch]^+[CNpyr]^-$: HBD mixtures, the evaporation rate is greatest whereas Ch±PhOH : HBD mixtures demonstrate the slowest and the smallest mass loss. This is not surprising considering the significant compacting of the liquid and the increased viscosities with Ch±PhOH systems as discussed later.

Physical properties

Density. Fig. 3 shows the measured densities and their linear fits to express the temperature dependence for each HBA : HBD (1 : 2) system. Table S2† shows the comparison of the experimentally measured and simulated densities at 25 °C, where the agreement is within ±6.5%. Density is an important property in general for estimating mass and footprint require-

 This journal is © The Royal Society of Chemistry 2024

Open Access Article. Published on 07 February 2024. Downloaded on 4/13/2026 5:23:57 AM.
This article is licensed under a Creative Commons Attribution-NonCommercial 3.0 Unported Licence.

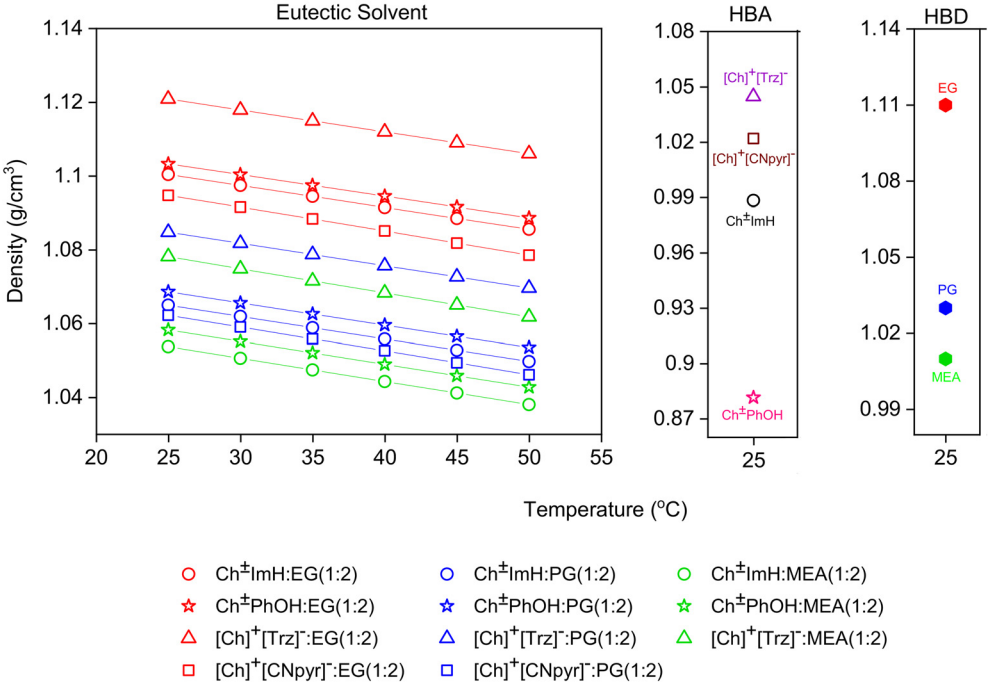

Fig. 3 Measured densities with respect to the temperature as a function of composition. The HBA and HBD densities at 25 °C are shown separately in side panels for clarity. The error in the measured densities of the liquid samples is smaller than the symbol, while the error of the solid HBAs is ±4%. The solid lines are linear fits (Table S3† lists the fit parameters).

ments in a given application utilizing these solvents (*e.g.*, calculation of gravimetric CO_2 absorption capacity). The measured densities of EG (1.11 g cm^{-3}), PG (1.03 g cm^{-3}), and MEA (1.01 g cm^{-3}) match perfectly with the reported densities for these HBDs.[31,32] When the eutectics with the same HBA are compared, both the experimental and simulation results demonstrate the solvents with EG as the HBD to have the largest densities, while those with MEA have the lowest, directly corresponding to the comparison between neat EG and MEA. Therefore, it can be said that HBD has a direct influence on the density. Table S3† lists the linear density fit parameters (and corresponding equation). Accordingly, the densities of HBA : MEA (1 : 2) eutectic solvents present higher dependence on temperature compared to those with EG and PG. Further, the density of eutectic solvents based on $[Ch]^+[CNpyr]^-$ have the greatest sensitivity to temperature whereas those based on PhOH have the least sensitivity, similar to the trends in the thermal stability of these solvents.

To examine the influence of the HBAs and HBDs on the nature of the intermolecular interactions occurring in these binary solvents, excess molar volume at 25 °C was calculated using the experimentally measured densities of the HBDs, HBAs, and eutectic solvents. As summarized in Table 2, negative excess molar volumes were obtained for all of the systems, indicating molecular packing due to the enhanced hydrogen bonding interactions compared to their pure component.[33] The largest deviation from ideal solution was observed with $Ch^{\pm}PhOH$: HBD mixtures, likely due to the π–π interactions induced in the liquid phase with the C_6 aromatic rings and the strong H-bonding induced by the PhOH alcohol conjugate group, differently than ImH, TrzH, and CNpyrH.

Table 2 Excess molar volumes (V_m^E) of the eutectic solvents, HBA : HBD (1 : 2), at 25 °C, as calculated using the measured densities

HBDs	HBAs	V_m^E (cm^3 mol^{-1})
EG	$Ch^{\pm}ImH$	−5.455
	$Ch^{\pm}PhOH$	−14.656
	$[Ch]^+[CNpyr]^-$	−3.589
	$[Ch]^+[Trz]^-$	−3.992
PG	$Ch^{\pm}ImH$	−5.489
	$Ch^{\pm}PhOH$	−14.681
	$[Ch]^+[CNpyr]^-$	−3.603
	$[Ch]^+[Trz]^-$	−4.227
MEA	$Ch^{\pm}ImH$	−5.192
	$Ch^{\pm}PhOH$	−14.222
	$[Ch]^+[Trz]^-$	−4.181

Viscosity and ionic conductivity. The measured viscosities of the eutectic solvents ranged between 643 mPa s for $Ch^{\pm}PhOH$: PG (1 : 2) and 96 mPa s for $[Ch]^+[CNpyr]^-$: EG (1 : 2) at 25 °C as seen in Fig. 4. Similar to the trends in viscosities, the ionic conductivity of $Ch^{\pm}PhOH$: EG was the lowest (0.36 mS cm^{-1}) and that of $[Ch]^+[CNpyr]^-$: EG (1 : 2) was the highest (2.28 mS cm^{-1}). Both PG and MEA-based solvents exhibited a similar trend, with the lowest conductivity observed in $Ch^{\pm}PhoH$ based eutectics, followed by $Ch^{\pm}ImH$, $[Ch]^+[Trz]^-$, and $[Ch]^+[CNpyr]^-$. This is not surprising considering the reduced ionic nature and increased viscosity in the case of $Ch^{\pm}ImH$ and $Ch^{\pm}PhOH$. The viscosities of neat HBDs are in perfect agreement with literature (18,[34] 44,[32] and 19,[35] mPa s

Open Access Article. Published on 07 February 2024. Downloaded on 4/13/2026 5:23:57 AM.
This article is licensed under a Creative Commons Attribution-NonCommercial 3.0 Unported Licence.

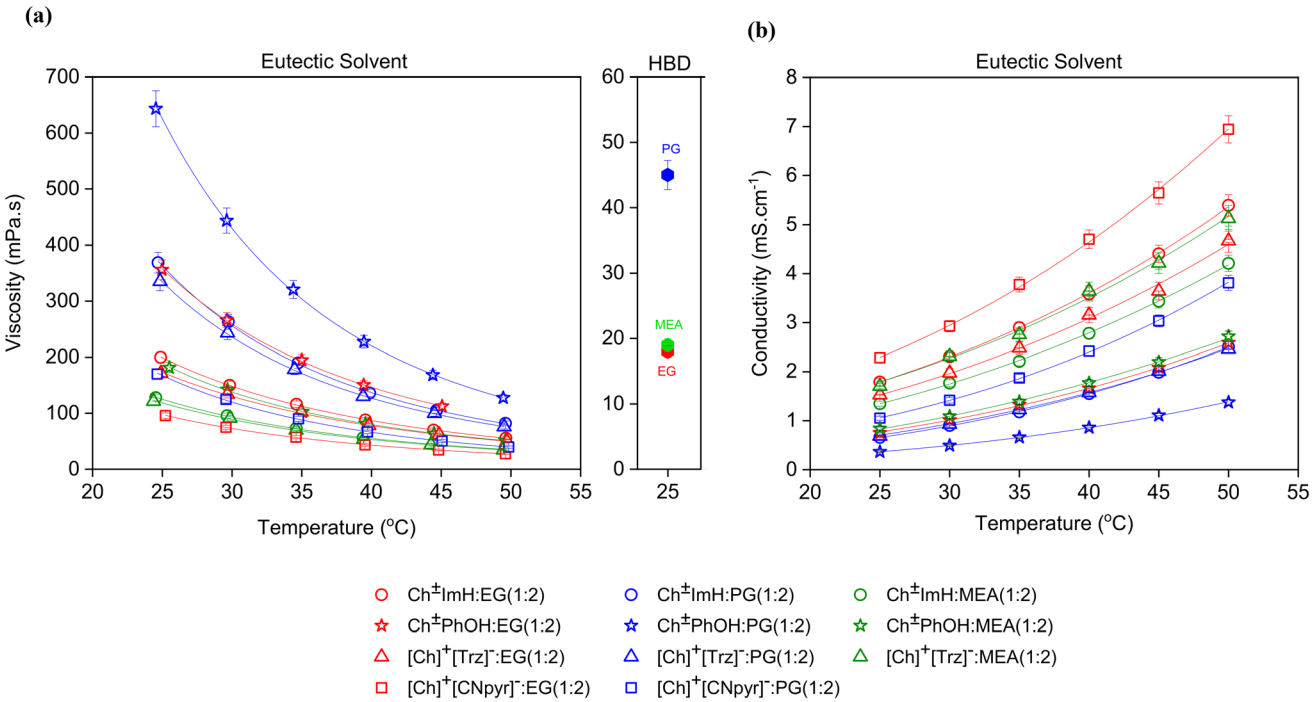

Fig. 4 Impact of the room temperature viscosities of the HBDs on the viscosity (a) and conductivity (b) of the eutectic solvents. Solid lines represent their VFT fits (fit parameters for viscosity and conductivity are shown in Tables S4 and S5,† respectively).

for EG, PG, and MEA, respectively). The temperature dependencies of viscosity and ionic conductivity are well described by the VFT model (solid lines in Fig. 4) hence the samples are characterized as glass forming liquids, consistent with observations by DSC. Overall, the viscosities are seen to primarily depend on the parent HBD in the case of EG and PG, consistent with a previous report on similar eutectic systems.[17] However, upon the replacement of EG with MEA (19 mPa s at 25 °C), a decrease in the viscosities of the eutectic solvents (about 2-fold) was observed. By replacing the hydroxyl functional group in EG with a primary amine group having a lower hydrogen bond donating ability, the strength of HBA–HBD interactions is weakened. This is supported by calculated hydrogen bonding (HB) statistics which show significantly more extensive hydrogen bonding with EG and PG than with MEA as seen in Fig. 5.

Hydrogen bonding (HB). Hydrogen bonding interactions between the HBA–HBD were observed *via* examining the OH proton shift in ^{1}H-NMR of the neat HBDs (Fig. S4†) and in the eutectic solvents (Fig. S5–S8†), where a general downshift of the OH proton in EG and PG was observed in all the HBA : HBD (1 : 2) mixtures examined. This downshift is indicative of a hydrogen bonding interaction that results in deshielding. These hydrogen bonding interactions were further analyzed with the MD simulations. The calculated HB statistics are presented in Fig. 5 (atom type notations are provided in Fig. S9†). Corresponding radial distribution functions (RDFs) are presented in Fig. S10.† Hydrogen bonding is highly system-dependent; however, the following generalizations can be made. First, all of the systems present significant HBD-HBD interactions (dark blue bars in Fig. 5). Second, HBs between the anion-HBD are the most significant for $[Ch]^+[Trz]^-$ (green bars). This stands true when comparing against $[Ch]^+[CNpyr]^-$: HBD (1 : 2) in which the interactions among the HBD molecules are the most significant instead. The stronger interactions in $[Ch]^+[Trz]^-$: HBD seen from MD simulations, both from the ionic and HB interactions, explain the higher viscosities measured. Third, in the case of neutral species, Ch$^{\pm}$ImH and Ch$^{\pm}$PhOH, interactions between Ch$^{\pm}$ and HBD are the most significant (labeled as cation-HBD; red bars in Fig. 5). It should be noted that since the proton sharing is not captured in MD simulations, for comparison arguments and simplicity in plotting, $[Ch]^+$ and Ch$^{\pm}$ are both referred as cations while PhOH and ImH are referred as anions in Fig. 5. Comparing hydrogen bonding results with experimentally measured properties, systems where cation-HBD interactions are dominant (*i.e.*, systems comprising Ch$^{\pm}$ImH and Ch$^{\pm}$PhOH) have larger viscosities and present larger deviations from ideal mixtures with respect to the excess molar volumes. Overall weaker HBA-HBD interactions (combination of red and green bars) in $[Ch]^+[CNpyr]^-$: HBD systems as obtained from MD simualtions further explain its relatively lower thermal stability and lower viscosity.

Solvatochromic analysis. The solvatochromic studies based on UV-vis absorbance probes provides key-insights of various solvent properties including the solvent polarity and their hydrogen bond accepting/donating ability. Betaine dyes represent a well-recognized class of solvatochromic absorbance probes and exhibits a pronounced negative solvatochromism with decrease in solvent polarity resulting in bathochromic

 This journal is © The Royal Society of Chemistry 2024

Open Access Article. Published on 07 February 2024. Downloaded on 4/13/2026 5:23:57 AM.
This article is licensed under a Creative Commons Attribution-NonCommercial 3.0 Unported Licence.

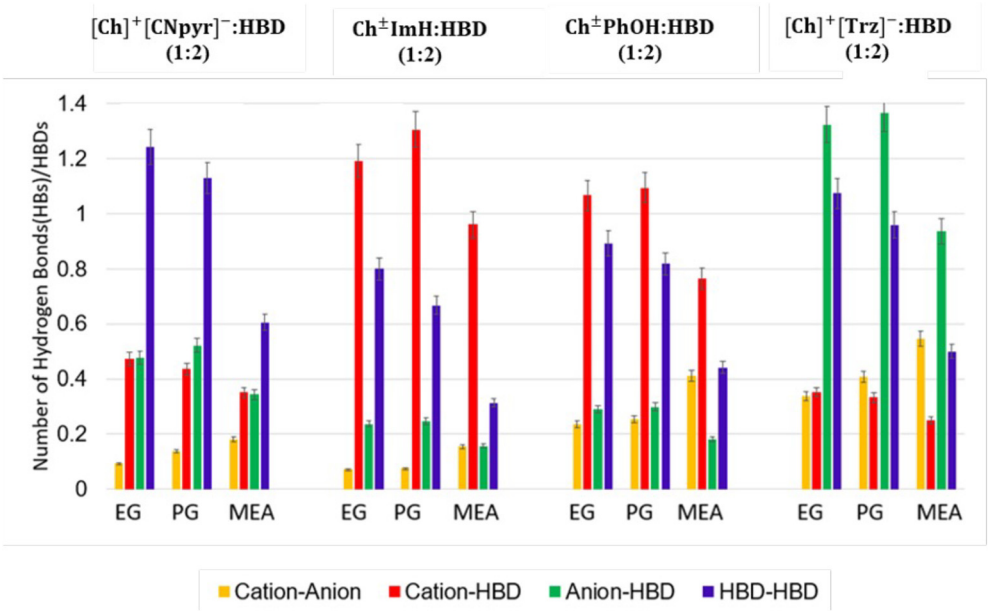

Fig. 5 Number of HBs per number of HBDs. Standard deviation in the number of hydrogen bonds was less than 10% in all the cases. (OH and NH groups are regarded as the donors, and the O and N groups the acceptors). The choline species $[Ch]^+$ and $Ch^{\pm}$ are both referred as cations for simplicity, and $[CNpyr]^-$, $[Trz]^-$, ImH and PhoH are referred as anions. EG, PG and MEA are the HBDs.

shift.[36,37] The spectral response of the dye is strongly affected by the solvent dipolarity/polarizability (π^*) and the hydrogen bond donating acidity (α). In this context, we have employed betaine 30 along with 4-nitroaniline (NA) and *N*,*N*-diethey-4-nitroaniline (DENA) to determine the solvent polarity $E_T(30)$ and Kamlet–Taft parameters, π^*, α and hydrogen bond acceptor basicity (β).[36–39] Kamlet–Taft parameters are widely used to establish the physicochemical properties of the eutectic solvents. The $E_T(30)$, π^*, α and β are evaluated from the absorbance maxima of the UV-vis probes and are listed in Table 3. A representative spectrum featuring the shift in absorbance response of the investigated UV-vis probes dissolved in eutectic mixtures of $[Ch]^+[Trz]^-$ with different HBDs is shown in Fig. S11.† The observed shifts in the absorbance maxima of the probes signifies the variations in the solvent environment. For both EG and PG, the highest $E_T(30)$ value is observed for the $[Ch]^+[CNpyr]^-$ mixtures trailed by the $[Ch]^+[Trz]^-$. The PhOH based mixtures showed lowest solvent polarities. The trend in the solvent polarities closely resembles the trend followed by the ionic conductivities and the decrease in viscosities of these mixtures. This supports the argument that the $[Ch]^+[CNpyr]^-$ and $[Ch]^+[Trz]^-$ has higher ionic character as compared to the $Ch^{\pm}$ImH and $Ch^{\pm}$PhOH-based solvents consisting of dipolar species imparting a greater polarizability to these solvents. The $E_T(30)$ value could not be determined for $Ch^{\pm}$ImH : MEA due to absence of the low energy-transition band for the dye. The Kamlet–Taft polarizability π^* value is largely similar for all the examined system and did not show any distinct trend. Whereas the β value was observed to be highest for the $Ch^{\pm}$ImH based eutectics indicating the greater tendency of the mixture to accept hydrogen bonding from the solute. The high basicity of these solvents can indicate their greater potential as CO_2 absorbing solvents. Subsequently, the acidity parameter α was determined by combining the responses of $E_T(30)$ and π^* which further shows the enhanced solvent-to-solute hydrogen bond donating capacity for the $[Ch]^+[CNpyr]^-$ HBA. These outcomes corroborate with MD simulations showing reduced interactions between the HBD and HBA resulting in the higher overall tendency of solvent to donate hydrogen bond towards the solute. The observed reduced HBD-HBA interactions for $[Ch]^+[CNpyr]^-$ HBA further rationalizes the lower thermal stability of these mixtures. For both hydroxyl functional based HBDs, the α follows the similar

Table 3 Kamlet–Taft parameters – dipolarity/polarizability (π^*), HBA basicity (β) HBD acidity (α), and $E_T(30)$ of the eutectic solvents at 298.15K. The standard error in π^*, β, and α are $\leq \pm 0.02$

Solvent HBA : HBD (1 : 2)	π^*	β	α	$E_T(30)$/ kcal mol^{-1}
$Ch^{\pm}$ImH : EG	1.11	0.83	0.72	54.98
$Ch^{\pm}$PhOH : EG*	N/A	N/A	N/A	54.56
$[Ch]^+[CNpyr]^-$: EG	1.13	0.77	0.77	56.28
$[Ch]^+[Trz]^-$: EG	1.11	0.60	0.75	55.62
$Ch^{\pm}$ImH : PG	1.09	0.88	0.68	54.15
$Ch^{\pm}$PhOH : PG*	N/A	N/A	N/A	54.15
$[Ch]^+[CNpyr]^-$: PG	1.09	0.74	0.78	55.84
$[Ch]^+[Trz]^-$: PG	1.06	0.64	0.76	54.87
$Ch^{\pm}$ImH : MEA	1.09	0.83	N/A	N/A
$Ch^{\pm}$PhOH : MEA*	N/A	N/A	N/A	51.05
$[Ch]^+[Trz]^-$: MEA	1.11	0.74	0.59	52.95

* Due to high absorbance of the PhOH-based systems, the spectral features were not well-resolved.

Open Access Article. Published on 07 February 2024. Downloaded on 4/13/2026 5:23:57 AM. This article is licensed under a Creative Commons Attribution-NonCommercial 3.0 Unported Licence.

trend, $[Ch]^+[CNpyr]^-$ > $[Ch]^+[Trz]^-$ > $Ch^{\pm}ImH$. The higher HBD acidity/polarity of these solvents can be considered as an indication of reduced nucleophilicity which impacts CO_2 binding as discussed later.

CO_2 absorption and impact on physical properties

CO_2 absorption in these eutectic solvents is through chemisorption, where CO_2 binds to the HBA and HBDs upon contact and releases at elevated temperatures (see Fig. S12†), as detailed in an earlier study by Dikki *et al.*[22] Accordingly, CO_2 primarily binds to the HBD (*i.e.*, EG-CO_2 accompanied with H-transfer to the anion/$Ch^{\pm}$). The measured CO_2 capacities and the changes in the viscosities and conductivities with CO_2 saturation are summarized in Table 4, along with a comparison to literature reporting these properties for similar solvents. The chemisorption process of CO_2 is generally accompanied by significant changes in the intermolecular interactions and possibly the liquid structure. The presence of chemisorbed CO_2 in HBA : HBD (1 : 2) eutectic solvents is shown by the appearance of the C=O and –COO vibrations in the FTIR spectra (Fig. S13 and S14†) that is otherwise absent in the neat solvents. The H-bonding enhanced by these absorption products underly the measured property changes in Table 4.

The change in viscosity and conductivity due to CO_2 absorption was significant as seen in Table 4 (Table S6† shows the increase in density that occurs upon CO_2 absorption). The largest positive change in viscosity, and consequently the largest reduction in conductivity among the systems investigated here was the $[Ch]^+[CNpyr]^-$ based eutectic solvents presenting the increased interactions with CO_2 absorption. While this increase in viscosity with CO_2 saturation is consistent with the trends observed in the literature data on similar solvents; it was not as dramatic (*e.g.*, previously reported examples in Table 4). There were also opposite trends; the largest reduction in viscosity was with the $Ch^{\pm}PhOH$ based eutectic solvents. The viscosity decrease is indicative of a weakened/disrupted intermolecular interaction post CO_2 chemisorption. In the case of the CO_2 reactive MEA, the eutectic solvent formed a gel and the viscosity could not be measured with the available instrument. It is also noteworthy that the eutectics composed of $[Ch]^+[Trz]^-$ exhibited smaller variations in both viscosity and conductivity upon CO_2 saturation.

A noticeable trend was seen between the measured solvent polarities and CO_2 absorption capacity. In general, PG based solvents showed an inverse correlation between the solvent polarity/acidity with their CO_2 absorbing capacities. Although, a definite trend is not observed for EG-based systems, a higher CO_2 absorption capacity is obtained for $Ch^{\pm}ImH$ and $Ch^{\pm}PhOH$ eutectics possessing lower HBD acidity/polarity. A similar correlation between the Kamlet–Taft parameters and CO_2 absorbing capacity is not observed for MEA based solvents. The presence of amine group renders it more nucleophilic towards the CO_2 compared to the hydroxy group-based systems.

Electrochemical stability

The electrochemical stability of the developed eutectic solvents was examined by cyclic voltammetry (CV) using a Pt microelectrode with a $Fc|Fc^+$ internal reference and a Pt quasi reference electrode (Fig. S15†). The high viscosity of the solvents necessitated the use of a microelectrode to overcome the mass transfer limitations. However, despite the use of a microelectrode,

Table 4 CO_2 capacity and change in the viscosities and conductivities of the eutectic solvents (HBA : HBD, 1 : 2) with CO_2 saturation at 1 bar CO_2 and 25 °C. Comparable systems from literature are included for comparison

		HBA : HBD (1 : 2)				
			Before CO_2 saturation		After CO_2 saturation	
HBDs	HBAs	CO_2 Capacity (mol kg^{-1})	Viscosity (mPa s)	Conductivity (mS cm^{-1})	Viscosity (mPa s)	Conductivity (mS cm^{-1})
EG	$Ch^{\pm}ImH$	3.25[22]	200	1.79	191	1.04
	$Ch^{\pm}PhOH$	2.49[22]	356	0.75	185	1.00
	$[Ch]^+[CNpyr]^-$	2.41[22]	95	2.28	178	1.11
	$[Ch]^+[Trz]^-$	2.36[22]	171	1.53	157	1.44
PG	$Ch^{\pm}ImH$	2.75	369	0.66	430	0.39
	$Ch^{\pm}PhOH$	2.35	644	0.36	409	0.42
	$[Ch]^+[CNpyr]^-$	1.72	170	1.05	340	0.47
	$[Ch]^+[Trz]^-$	2.03	335	0.69	349	0.54
MEA	$Ch^{\pm}ImH$	4.60	128	1.35	N/A	0.04
	$Ch^{\pm}PhOH$	3.13	182	0.84	N/A	N/A
	$[Ch]^+[Trz]^-$	4.92	121	1.71	N/A	0.04
Examples of prior reports						
[a]EG[20]	$[EMIM]^+[CNPyr]^-$	2.59	45	—	88	—
[b]EG[40]	$[HDBU]^+[Im]^-$	3.20	31.48	—	166.51	—
[c]none[41]	$[P_{66614}]^+[CNpyr]^-$	1.55	360	—	370	—
[d]DEA[42]	$[MEAH]^+[Cl]^-$	2.64	262	—	~1500	—
[e]MEA[43]	$[Ch]^+[Ch]^-$	6.18	~25	—	—	—

[a] $[EMIM]^+$ = 1-ethyl,3-methylimidazolium. [b] $[HDBU]^+[Im]^-$ = 1,8-diazabicyclo[5,4,0]undec-7-ene imidazole; HBA : HBD (7 : 3) at 40 °C. [c] $[P_{66614}]^+$ = Trihexyl(tetradecyl)phosphonium. [d] MDEA = *N*-methyldiethanolamine; $[MEAH]^+[Cl]^-$ = Monoethanolamine hydrochloride; HBA : HBD (1 : 3). [e] MEA = Monoethaolamine; HBA : HBD (1 : 5) at 30 °C.

 This journal is © The Royal Society of Chemistry 2024

Open Access Article. Published on 07 February 2024. Downloaded on 4/13/2026 5:23:57 AM.
This article is licensed under a Creative Commons Attribution-NonCommercial 3.0 Unported Licence.

limitations persisted as of $Fc|Fc^+$ redox peaks were only discernible when scan rate was increased from 10 mV s^{-1} to 1 V s^{-1} (Fig. S16†). While the Fc redox reaction is considered as representative outer-sphere redox reaction that do not specifically interact with the electrode surface,[44] it is a well-known phenomenon that eutectic solvents components are prone to adsorption on the electrode surface,[45,46] even controlling the differential capacitance behavior of the electrode–electrolyte interface.[47] In addition, the anodic limit was difficult to observe since no significant current occurred with increased positive polarization. However, an oxidation peak at +0.9 V *vs.* $Fc|Fc^+$ was seen. This is attributed to deposition of the electrolyte breakdown species and deactivation of the electrode that can explain the lack of any significant anodic current. On the other hand, all samples displayed a similar onset potential (−1.24 to −1.43 V) for the cathodic end, indicating that this behavior is likely predominantly governed by the reduction of choline species as the common component. However, the cathodic current followed the trends in bulk viscosities and conductivities; those with PG and MEA resulting in the lowest currents. Accordingly, the electrochemical stability windows on Pt are estimated to be between −2.1 to −2.3 V, hence these solvents could be considered for electrochemical conversion of the captured CO_2, specifically when further diluted in aprotic solvents for increased rates.

QSPR analysis for prediction of viscosity and CO_2 absorption capacities

QSPR analysis is a simple tool that correlates and enables prediction of physicochemical properties of compounds through mathematical models based on their molecular structural descriptors, thereby facilitating time and cost-effective discovery of new materials and optimization of existing ones. Thus, to elucidate the correlation between theoretical structural descriptors of HBAs and HBDs, and experimental properties of eutectic solvents such as viscosity, density, and CO_2 capacity, QSPR analysis was performed. A total of 15 different structural descriptors were chosen for each cation, anion, and diluent, summarized in Tables S7 and S8.† First, ERM algorithm in MATLAB was employed to find the optimal set of structural descriptors among the dataset of 45 descriptors to correlate the experimental properties (viscosity and CO_2 capacity) of eutectic solvents, as these two are critical for CO_2 capture application. Among the total of 45 descriptors, QSPR analysis identified a set of five descriptors as the primary structural parameters determining the viscosity and CO_2 capacity of eutectic solvents. Following this, multi-linear regression model (MLR) was performed for each property to obtain the best fit linear models that correlates the identified descriptors and the viscosity and CO_2 capacity of eutectic solvents along with regression parameters as expressed by eqn (1) and (2), respectively.

$$\begin{aligned}\text{Viscosity}_{(\text{mPa s})} &= 28754.501 - 199.983 \times \text{CPK Area}_{\text{cation}} \\ &\quad + 4.977 \times \text{CPK Volume}_{\text{anion}} + 312.872 \\ &\quad \times \text{HBA Count}_{\text{anion}} + 791.741 \\ &\quad \times \text{CPK Volume}_{\text{diluent}} - 893.136 \times \text{Cv}_{\text{diluent}}\end{aligned} \tag{1}$$

$$\begin{aligned}\text{CO}_2\text{ Capacity}_{(\text{mol kg}^{-1})} &= -0.057 - 2.033 \times \text{E LUMO}_{\text{cation}} \\ &\quad - 1.299 \times \text{E LUMO}_{\text{anion}} + 0.108 \\ &\quad \times \text{ Polarizabilty}_{\text{anion}} + 7.911 \\ &\quad \times \text{E LUMO}_{\text{diluent}} - 0.017 \times \text{CPK Area}_{\text{diluent}}\end{aligned} \tag{2}$$

Fig. 6 demonstrate the correlation between the experimental and calculated values of viscosity and CO_2 capacity of eutectic solvents using QSPR model. Fig. 6a shows an excellent correlation between the experimental and calculated viscosities of eutectic solvents in terms of goodness of prediction (R^2 = 0.99). Fig. 6b shows a slightly lower, but still acceptable, correlation (R^2 = 0.63) between the experimental and predicted CO_2 capacities of eutectic solvents. To further validate the pre-

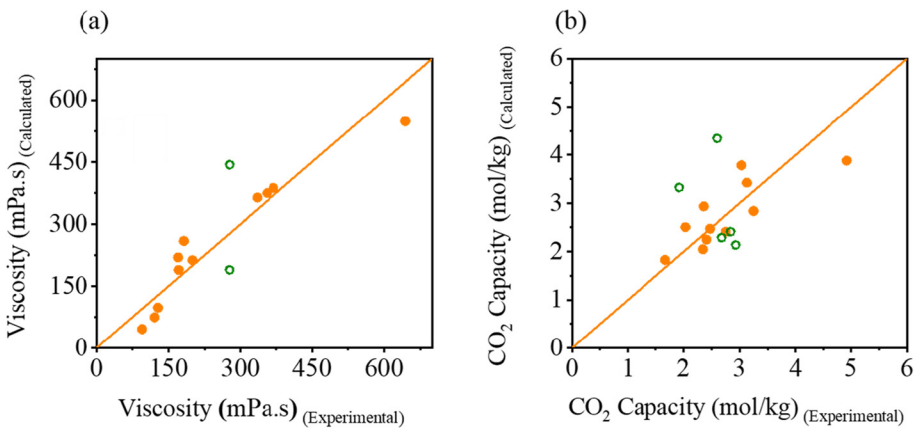

Fig. 6 Comparison between experimental and predicted values of the viscosity (a) and CO_2 gravimetric capacity (b) of the eutectic solvents. Hollow symbols represent comparison between experimental data for different eutectic solvents obtained from literature and those predicted by the MLR model.

Open Access Article. Published on 07 February 2024. Downloaded on 4/13/2026 5:23:57 AM.
This article is licensed under a Creative Commons Attribution-NonCommercial 3.0 Unported Licence.

diction capability of the model, additional experimental viscosity and CO_2 capacity values of other eutectic solvents reported in the literature were checked.[20,21,48] Specifically, the structural descriptors were calculated (summarized in Table S8†) and used in eqn (1) and (2) to predict viscosities and CO_2 capacities. The predicted values demonstrated a reasonably good agreement with experimental values, which further demonstrate the utility of these models for a first estimation. We also performed MLR for density data to obtain the best fit linear model (eqn (S12)†) that correlates the experimental and calculated values of density of eutectic solvents. Similarly, model exhibited excellent correlation between the predicted and experimental densities of eutectic solvents (R^2 = 0.90). However, the correlation between experimental density data obtained from literature and predicted values by our model was notably poor, as shown in Fig. S17.† The primary reason for the relatively poor predictions of the QSPR model is the limited literature data that comes from DESs with a narrow structural diversity used to train the models (*i.e.*, one cation, four anions, and three hydrogen bond doners). Furthermore, the IL descriptors used in the QSPR analysis were calculated separately for the cation and anion for simplicity; however, in practice, the cation and anion of the IL should be considered together (proton sharing could not be captured in descriptors). Therefore, calculation of IL descriptors should also make significant contribution to the error of QSPR models. In order to further improve the predictive capability of the QSPR model, future studies should focus on expanding the dataset by including a wide range of eutectic solvents and evaluate the models under different testing conditions such as varied moisture, temperature, and pressure. This will improve optimization of eutectic solvent properties for specific applications.

Conclusion

In summary, choline based eutectic solvents containing imidazole, phenol, pyrrole-2-carbonitrile, and 1,2,4-triazole based HBAs were investigated with alcohol/amine-based HBDs including ethylene glycol, 1,2-propylene glycol, and monoethanolamine. The thermal, physical, electrochemical, and solvatochromic properties of the eutectic solvents formed was observed to depend strongly on the HBD and the HBA-HBD interactions. With CO_2 saturation, the viscosities had an overall increase, except for interestingly the phenol based eutectic solvents. Phenol HBA based solvents with EG and PG HBDs experienced significant decrease in viscosity upon CO_2 saturation, whereas the pyrrole-2-carbonitrile based solvents experienced an increase in viscosity. These contrasting trends are attributed to the robustness of the intermolecular interactions where a weakening occurs with chemisorbed CO_2 in phenol-based eutectics. The monoethanolamine based eutectic solvents in general possessed lower viscosity and decreased thermal stability owing to the decreased hydrogen bond donating ability of the amine compared to other solvents studied; however, a gel like material was obtained after saturation with CO_2 due to significantly increased H-bonding. Finally, multi linear regression analysis was performed to identify simple molecular descriptors for estimating physical properties, in particular for viscosity and CO_2 capacities that can inform future designs of green eutectic solvents for reactive CO_2 capture and electrochemical conversion processes.

Author contributions

R. D. performed the physical property measurements, thermal analysis, and CO_2 absorption experiments. V. K. performed solvatochromic studies and ionic conductivities. M. Z. performed QSPR analysis. S. B. performed MD simulations and structural analysis. O. K. C. performed electrochemical stability measurements. R. G. developed the computational plan and oversaw simulation discussions. B. G. developed the experimental plan, oversaw the analysis, and managed the project. All authors contributed to the writing and editing of the manuscript.

Conflicts of interest

There are no conflicts to declare.

Acknowledgements

This study was supported by the U.S. Department of Energy, Office of Science, Basic Energy Sciences under award number DE-SC0022214. Authors acknowledge partial support from U.S. Department of Energy, Office of Science, Energy Frontier Research Centers, under award number DE-SC0023427; granted to Center for Closing the Carbon Cycle (4C) for conductivity measurements and electrochemical characterization. Authors thank Northeast Ohio High Field NMR Facility and the Department of Chemistry for access to NMR.

References

1 B. Gurkan, H. Squire and E. Pentzer, Metal-Free Deep Eutectic Solvents: Preparation, Physical Properties, and Significance, *J. Phys. Chem. Lett.*, 2019, **10**(24), 7956–7964, DOI: 10.1021/acs.jpclett.9b01980.

2 C. Florindo, F. Lima, B. D. Ribeiro and I. M. Marrucho, Deep Eutectic Solvents: Overcoming 21st Century Challenges, *Curr. Opin. Green Sustainable Chem.*, 2019, **18**, 31–36, DOI: 10.1016/j.cogsc.2018.12.003.

3 Q. Zaib, M. J. Eckelman, Y. Yang and D. Kyung, Are Deep Eutectic Solvents Really Green?: A Life-Cycle Perspective, *Green Chem.*, 2022, **24**(20), 7924–7930, DOI: 10.1039/D2GC01752K.

4 A. Van Den Bruinhorst and M. C. Gomes, Is There Depth to Eutectic Solvents?, *Curr. Opin. Green Sustainable Chem.*, 2022, **37**, 100659, DOI: 10.1016/j.cogsc.2022.100659.

 This journal is © The Royal Society of Chemistry 2024

Open Access Article. Published on 07 February 2024. Downloaded on 4/13/2026 5:23:57 AM. This article is licensed under a Creative Commons Attribution-NonCommercial 3.0 Unported Licence.

5 R. Ghahremani, R. F. Savinell and B. Gurkan, Perspective—Hydrogen Bonded Concentrated Electrolytes for Redox Flow Batteries: Limitations and Prospects, *J. Electrochem. Soc.*, 2022, **169**(3), 030520, DOI: 10.1149/1945-7111/ac58c6.

6 R. Ghahremani, W. Dean, N. Sinclair, X. Shen, N. Starvaggi, I. Alfurayj, C. Burda, E. Pentzer, J. Wainright and R. Savinell, Gurkan, B. Redox-Active Eutectic Electrolyte with Viologen and Ferrocene Derivatives for Flow Batteries, *ACS Appl. Mater. Interfaces*, 2022, **15**(1), 1148–1156, DOI: 10.1021/acsami.2c18546.

7 M. H. Nematollahi and P. J. Carvalho, Green Solvents for CO_2 Capture, *Curr. Opin. Green Sustainable Chem.*, 2019, **18**, 25–30, DOI: 10.1016/j.cogsc.2018.11.012.

8 C. Ma, N. Wang, Y. Xie and X. Ji, Hybrid Solvents Based on Ionic Liquids/Deep Eutectic Solvents for CO_2 Separation, *Sci. Talks*, 2023, **6**, 100220, DOI: 10.1016/j.sctalk.2023.100220.

9 S. Imteyaz, C. M. Suresh, T. Kausar and P. P. Ingole, Carbon Dioxide Capture and Its Electrochemical Reduction Study in Deep Eutectic Solvent (DES) via Experimental and Molecular Simulation Approaches, *J. CO_2 Util.*, 2023, **68**, 102349, DOI: 10.1016/j.jcou.2022.102349.

10 Y. Xu, R. Zhang, Y. Zhou, D. Hu, C. Ge, W. Fan, B. Chen, Y. Chen, W. Zhang, H. Liu, G. Cui and H. Lu, Tuning Ionic Liquid-Based Functional Deep Eutectic Solvents and Other Functional Mixtures for CO_2 Capture, *Chem. Eng. J.*, 2023, **463**, 142298, DOI: 10.1016/j.cej.2023.142298.

11 J. Jo, J. Park, S. Kwon, M. Park, J. Jung, Y. Yoo and D. Kang, Journal of Environmental Chemical Engineering Revolutionizing CO2 Capture: Molecular Complexes of Deep Eutectic Solvents with Enhanced Hydrogen Bond Accepting Interaction for Superior Absorption Performance, *J. Environ. Chem. Eng.*, 2023, **11**(3), 110108, DOI: 10.1016/j.jece.2023.110108.

12 M. Zeeshan, M. K. Kidder, E. Pentzer, R. B. Getman and B. Gurkan, Direct Air Capture of CO_2: From Insights into the Current and Emerging Approaches to Future Opportunities, *Front. Sustain.*, 2023, **4**, 1167713, DOI: 10.3389/frsus.2023.1167713.

13 T. Lemaoui, A. S. Darwish, A. Attoui, F. Abu Hatab, N. E. H. Hammoudi, Y. Benguerba, L. F. Vega and I. M. Alnashef, Predicting the Density and Viscosity of Hydrophobic Eutectic Solvents: Towards the Development of Sustainable Solvents, *Green Chem.*, 2020, **22**(23), 8511–8530, DOI: 10.1039/D0GC03077E.

14 T. J. Trivedi, J. H. Lee, H. J. Lee, Y. K. Jeong and J. W. Choi, Deep Eutectic Solvents as Attractive Media for CO_2 Capture, *Green Chem.*, 2016, **18**(9), 2834–2842, DOI: 10.1039/C5GC02319J.

15 M. Mohan, O. Demerdash, B. A. Simmons, J. C. Smith, M. K. Kidder and S. Singh, Accurate Prediction of Carbon Dioxide Capture by Deep Eutectic Solvents Using Quantum Chemistry and a Neural Network, *Green Chem.*, 2023, **25**(9), 3475–3492, DOI: 10.1039/D2GC04425K.

16 J. Ruan, L. Chen and Z. Qi, Deep Eutectic Solvents as a Versatile Platform toward CO2 Capture and Utilization, *Green Chem.*, 2023, **25**(21), 8328–8348, DOI: 10.1039/D3GC02468G.

17 V. P. Cotroneo-figueroa, P. Aravena, V. Vesovic and R. I. Canales, Viscosity of Choline Chloride-Based Deep Eutectic Solvents: Experiments and Modeling, *J. Chem. Eng. Data*, 2020, **65**, 5581–5592, DOI: 10.1021/acs.jced.0c00715.

18 S. Spittle, D. Poe, B. Doherty, C. Kolodziej, L. Heroux, A. Haque, H. Squire, T. Cosby, Y. Zhang, C. Fraenza, S. Bhattacharyya, M. Tyagi, J. Peng, R. A. Elgammal, T. Zawodzinski, M. Tuckerman, S. Greenbaum, B. Gurkan, C. Burda, M. Dadmun, E. J. Maginn and J. Sangoro, Evolution of Microscopic Heterogeneity and Dynamics in Choline Chloride-Based Deep Eutectic Solvents, *Nat. Commun.*, 2022, **13**, 219, DOI: 10.1038/s41467-021-27842-z.

19 Y. Chen, X. Hu, W. Chen, C. Liu and K. Qiao, High Volatility of Superbase-Derived Eutectic, *Phys. Chem. Chem. Phys.*, 2021, 2193–2210, DOI: 10.1039/d0cp05885h.

20 Y. Lee, D. Penley, A. Klemm, W. Dean and B. Gurkan, Deep Eutectic Solvent Formed by Imidazolium Cyanopyrrolide and Ethylene Glycol for Reactive CO2 Separations, *ACS Sustainable Chem. Eng.*, 2021, **9**, 1090–1098, DOI: 10.1021/acssuschemeng.0c07217.

21 A. Klemm, S. P. Vicchio, S. Bhattacharjee, E. Cagli, Y. Park, M. Zeeshan, R. Dikki, H. Liu, M. K. Kidder, R. B. Getman and B. Gurkan, Impact of Hydrogen Bonds on CO2 Binding in Eutectic Solvents: An Experimental and Computational Study toward Sorbent Design for CO_2 Capture, *ACS Sustainable Chem. Eng.*, 2023, **11**, 3740–3749, DOI: 10.1021/acssuschemeng.2c06767.

22 R. Dikki, E. Cagli, D. Penley, M. Karayilan and B. Gurkan, Formation of Choline Salts and Dipolar Ions for CO2 Reactive Eutectic Solvents, *Chem. Commun.*, 2023, **59**(80), 12027–12030, DOI: 10.1039/D3CC03272H.

23 C. Schick, Differential Scanning Calorimetry (DSC) of Semicrystalline Polymers, *Anal. Bioanal. Chem.*, 2009, **395**, 1589–1611, DOI: 10.1007/s00216-009-3169-y.

24 E. Ikada, Y. Hida, H. Okamoto, J. Hagino and N. Koizumi, Dielectric Properties of Ethanolamines, *Bull. Inst. Chem. Res., Kyoto Univ.*, 1968, **46**(5), 239–247.

25 C. A. Taylor and W. H. Rinkenbach, Ethylene Glycol: An Evaluation of Avaiblable Information on the Physical Properties of This Compound, *Ind. Eng. Chem.*, 1926, **18**(7), 676–678, DOI: 10.1016/B978-0-323-89773-0.00040-0.

26 D. R. Lide, *CRC Handbook of Chemistry and Physics*, CRC press, Taylor & Francis Boca Raton, 2008.

27 Y. Y. Lee, K. Edgehouse, A. Klemm, H. Mao, E. Pentzer and B. Gurkan, Capsules of Reactive Ionic Liquids for Selective Capture of Carbon Dioxide at Low Concentrations, *ACS Appl. Mater. Interfaces*, 2020, **12**(16), 19184–19193, DOI: 10.1021/acsami.0c01622.

28 P. D. Jadhav, R. V. Chatti, R. B. Biniwale, N. K. Labhsetwar, S. Devotta and S. S. Rayalu, Monoethanol Amine Modified Zeolite 13X for CO2 Adsorption at Different Temperatures, *Energy Fuels*, 2007, **21**, 3555–3559.

29 F. He, N. Wu, Z. Zhou and J. Wang, Experimental Investigation on Transpiration Cooling Using Propylene

Open Access Article. Published on 07 February 2024. Downloaded on 4/13/2026 5:23:57 AM.
This article is licensed under a Creative Commons Attribution-NonCommercial 3.0 Unported Licence.

Glycol Aqueous Solution, *Int. J. Therm. Sci.*, 2021, **164**, 106890, DOI: 10.1016/j.ijthermalsci.2021.106890.

30 G. O. Curme Jr. and C. O. Young, Ethylene Glycol: A Contribution of Chemistry to the Automobile Antifreeze Problem, *Ind. Eng. Chem.*, 1925, 1117–1120.

31 G. MacBeth and A. R. Thompson, Densities and Refractive Indexes for Ethylene Glycol-Water Solutions, *Anal. Chem.*, 1951, **23**(4), 618–619, DOI: 10.1021/ac60052a019.

32 D. I. Sagdeev, M. G. Fomina and I. M. Abdulagatov, Density and Viscosity of Propylene Glycol at High Temperatures and High Pressures, *Fluid Phase Equilib.*, 2017, **450**, 99–111, DOI: 10.1016/j.fluid.2017.07.006.

33 I. Bahadur, T. M. Letcher, S. Singh, G. G. Redhi, P. Venkatesu and D. Ramjugernath, Excess Molar Volumes of Binary Mixtures (an Ionic Liquid + Water): A Review, *J. Chem. Thermodyn.*, 2015, **82**, 34–46, DOI: 10.1016/j.jct.2014.10.003.

34 Z. Said, N. K. Cakmak, P. Sharma, L. S. Sundar, A. Inayat, O. Keklikcioglu and C. Li, Synthesis, Stability, Density, Viscosity of Ethylene Glycol-Based Ternary Hybrid Nanofluids: Experimental Investigations and Model -Prediction Using Modern Machine Learning Techniques, *Powder Technol.*, 2022, **400**, 117190, DOI: 10.1016/j.powtec.2022.117190.

35 U. S. P. R. Arachchige, N. Aryal, D. A. Eimer and M. C. Melaaen, Viscosities of Pure and Aqueous Solutions of Monoethanolamine (MEA), Diethanolamine (DEA) and n-Methyldiethanolamine (MDEA), *Annu. Trans. - Nord. Rheol. Soc.*, 2013, **21**, 299–306.

36 C. Reichardt, Solvatochromic Dyes as Solvent Polarity Indicators, *Chem. Rev.*, 1994, **94**, 2319–2358, DOI: 10.1021/cr00032a005.

37 C. Reichardt, *Solvents and Solvent Effects in Organic Chemistry*, Wiley, 2003, DOI: 10.1002/3527601791.

38 H. Model, The Solvatochromic Comparison Method. 2. The Ce-Scale of Solvent Hydrogen-Bond Donor (HBD) Acidities, *J. Am. Chem. Soc.*, 1976, 2886–2894.

39 M. H. Abraham and R. W. Taft, Linear Solvation Energy Relationships. 23. A Comprehensive Collection of the Solvatochromic Parameters, Π*, a, and p, and Some Methods for Simplifying the Generalized Solvatochromic Equation, *J. Org. Chem.*, 1983, **13**, 2877–2887.

40 H. Yan, L. Zhao, Y. Bai, F. Li, H. Dong, H. Wang, X. Zhang and S. Zeng, Superbase Ionic Liquid-Based Deep Eutectic Solvents for Improving CO_2 Absorption, *ACS Sustainable Chem. Eng.*, 2020, **8**, 2523–2530, DOI: 10.1021/acssuschemeng.9b07128.

41 B. Gurkan, B. F. Goodrich, E. M. Mindrup, L. E. Ficke, M. Massel, S. Seo, T. P. Senftle, H. Wu, M. F. Glaser, J. K. Shah, E. J. Maginn, J. F. Brennecke and W. F. Schneider, Molecular Design of High Capacity, Low Viscosity, Chemically Tunable Ionic Liquids for CO_2 Capture, *J. Phys. Chem. Lett.*, 2010, **1**(24), 3494–3499, DOI: 10.1021/jz101533k.

42 N. Ahmad, X. Lin, X. Wang, J. Xu and X. Xu, Understanding the CO_2 Capture Performance by MDEA-Based Deep Eutectics Solvents with Excellent Cyclic Capacity, *Fuel*, 2021, **293**(59), 120466, DOI: 10.1016/j.fuel.2021.120466.

43 X. Liu, Q. Ao, S. Shi and S. Li, CO2 Capture by Alcohol Ammonia Based Deep Eutectic Solvents with Different Water Content, *Mater. Res. Express*, 2022, **9**(1), 015504, DOI: 10.1088/2053-1591/ac47c6.

44 N. Kurapati, P. Pathirathna, C. J. Ziegler and S. Amemiya, Adsorption and Electron-Transfer Mechanisms of Ferrocene Carboxylates and Sulfonates at Highly Oriented Pyrolytic Graphite, *ChemSystemsChem*, 2019, **6**, 5651–5660, DOI: 10.1002/celc.201901664.

45 R. Costa, M. Figueiredo, C. M. Pereira and F. Silva, Electrochimica Acta Electrochemical Double Layer at the Interfaces of Hg/Choline Chloride Based Solvents, *Electrochim. Acta*, 2010, **55**(28), 8916–8920, DOI: 10.1016/j.electacta.2010.07.070.

46 Z. Chen, B. Mclean, M. Ludwig, R. Stefanovic, G. G. Warr, G. B. Webber, A. J. Page and R. Atkin, Interfaces as a Function of Potential, *J. Phys. Chem. C*, 2016, **120**, 2225–2233, DOI: 10.1021/acs.jpcc.5b10624.

47 W. Dean, J. Klein and B. Gurkan, Do Deep Eutectic Solvents Behave like Ionic Liquid Electrolytes? A Perspective from the Electrode-Electrolyte Interface, *J. Electrochem. Soc.*, 2021, **168**, 026503, DOI: 10.1149/1945-7111/abde83.

48 G. Cui, M. Lv and D. Yang, Efficient CO_2 Absorption by Azolide-Based Deep Eutectic Solvents, *Chem. Commun.*, 2019, 1426–1429, DOI: 10.1039/c8cc10085c.

This journal is © The Royal Society of Chemistry 2024